

Kinetic, Isotherm and Thermodynamic Analysis on Adsorption of Cr(VI) Ions from Aqueous Solutions by Synthesis and Characterization of Magnetic-Poly (divinylbenzene-vinylimidazole) Microbeads

Ali Kara · Emel Demirbel

Received: 23 June 2011 / Accepted: 24 November 2011 / Published online: 16 December 2011
© The Author(s) 2011. This article is published with open access at Springerlink.com

Abstract The magnetic-poly(divinylbenzene-1-vinylimidazole) [m-poly(DVB-VIM)] microbeads (average diameter 53–212 μm) were synthesized and characterized; their use as adsorbent in removal of Cr(VI) ions from aqueous solutions was investigated. The m-poly(DVB-VIM) microbeads were prepared by copolymerizing of divinylbenzene (DVB) with 1-vinylimidazole (VIM). The m-poly(DVB-VIM) microbeads were characterized by N_2 adsorption/desorption isotherms, ESR, elemental analysis, scanning electron microscope (SEM) and swelling studies. At fixed solid/solution ratio the various factors affecting adsorption of Cr(VI) ions from aqueous solutions such as pH, initial concentration, contact time and temperature were analyzed. Langmuir, Freundlich and Dubinin–Radushkovich isotherms were used as the model adsorption equilibrium data. Langmuir isotherm model was the most adequate. The pseudo-first-order, pseudo-second-order, Ritch-second-order and intraparticle diffusion models were used to describe the adsorption kinetics. The apparent activation energy was found to be $5.024 \text{ kJ mol}^{-1}$, which is characteristic of a chemically controlled reaction. The experimental data fitted to pseudo-second-order kinetic. The study of temperature effect was quantified by calculating various thermodynamic parameters such as Gibbs free energy,

enthalpy and entropy changes. The thermodynamic parameters obtained indicated the endothermic nature of adsorption of Cr(VI) ions. Moreover, after the use in adsorption, the m-poly(DVB-VIM) microbeads with paramagnetic property were separated via the applied magnetic force. The magnetic beads could be desorbed up to about 97% by treating with 1.0 M NaOH. These features make the m-poly(DVB-VIM) microbeads a potential candidate for support of Cr(VI) ions removal under magnetic field.

Keywords Magnetic polymers · Adsorption isotherm · Adsorption kinetic · Adsorption thermodynamic · Cr (VI) ions

Abbreviations

C_e	Concentration of Cr(VI) ions at equilibrium (mg L^{-1})
C_0	Initial concentration of Cr(VI) ions in solution of Cr(VI) ions (mg L^{-1})
E_a	Activation energy of adsorption (kJ mol^{-1})
E_{fe}	Free energy of adsorption (kJ mol^{-1})
ΔG	Gibbs free energy of adsorption (J mol^{-1})
ΔH	Isosteric enthalpy of adsorption (J mol^{-1})
ΔS	Entropy change of the adsorption process ($\text{J mol}^{-1} \text{K}^{-1}$)
q_e	The amount of Cr(VI) ions adsorbed on the adsorbent at equilibrium (mg g^{-1})
q_t	The amount of Cr(VI) ions adsorbed on the adsorbent at any time (mg g^{-1})

A. Kara (✉) · E. Demirbel
Department of Chemistry, Uludag University,
Bursa, Turkey
e-mail: akara@uludag.edu.tr

q_m	The maximum amount of Cr(VI) ions adsorbed per unit mass adsorbent (mg g^{-1})
Q_L	The maximum amount of Cr(VI) ions adsorbed per unit mass adsorbent (mg g^{-1})
K_L	The Langmuir constant related to the affinity of binding sites (mL mg^{-1})
n	The heterogeneity factor
K_F	The Freundlich constant
Q_{D-R}	The maximum amount of Cr(VI) ions adsorbed per unit mass adsorbent (mg g^{-1})
K_{D-R}	The Dubinin–Radushkevich constant ($\text{mol}^2 \text{J}^{-2}$)
ε	The polanyi potential (J mol^{-1})
R_L	The dimensionless separation factor
k_1	The rate constant of pseudo first-order adsorption (min^{-1})
k_2	The rate constant of pseudo second-order adsorption ($(\text{g/mg}) \text{min}^{-1}$)
k_R	The rate constant for the modified Ritchie's-second-order model (min^{-1})
k_i	The intraparticle diffusion rate constant ($\text{mg/g min}^{0.5}$)
R^2	Linear regression coefficient
t	Time (min)
T	Temperature (K)

1 Introduction

Chromium has applications in a variety of industries for industrial growth of any society. It is frequently used in leather tanning, pigment manufacture, textile and dyeing, and makes an important component for a number of alloys (Hena 2010). Although the most common oxidation states of chromium are from +2 to +6, two states, +3 and +6, are of environmental significance. Cr(VI) ions are 500 times more toxic than the trivalent one, and because of Cr(VI)'s mutagenic and carcinogenic properties, Cr(VI) includes skin irritation to lung cancer, as well as kidney, liver and gastric damage (Mansri et al. 2009). Several treatment processes have been in practice for removal of Cr(VI) ions from water and wastewater. Reduction of Cr(VI) ions to Cr(III) ions by a reducing agent and precipitation of chromium by pH adjustment has been quite popular (Fiol et al. 2008). Removal of Cr(VI) by adsorption onto polymer has been a popular choice in the developed world (Owlad et al. 2009). Polymeric adsorbents produced the desired forms (bead, membran,

etc.) find a wide range of applications for the removal of Cr(VI) due to their economical advantages, high efficiency, easy handling, and reusability (Uzdoğan et al. 2010).

The removal of heavy metal ions such as Cr(VI) with metal chelating polymers, a class of polymeric adsorbents, forming agent or some copolymers in the form of polymeric beads would be of great importance in environmental applications (Uğuzdoğan et al. 2009). Several criteria are important in the design of metal-chelating polymers with substantial stability for the selective removal of metal ions, including specific and fast complexation of the metal ions (Rivas et al. 2000; Kantipuly et al. 1990). Polymeric adsorbents incorporated with dithiocarbamate (Say et al. 2006; Pişkin et al. 1996), dithizone (Salih et al. 1998), vinyl pyridine (Duran et al. 2008), phenylenediamine (Li et al. 2009; Lu et al. 2007), chitosan (Copello et al. 2008), vinyl imidazole (Kara et al. 2004; Fontanals et al. 2004), diethylenetriamine (Liu et al. 2006), *N*-methacryloylhistidine (Say et al. 2006), poly(ethyleneimine) (Bayramoğlu and Arica 2005; Say et al. 2002a, b), salicylaldehyde (Ebraheem and Hamdi 1997), tannic acid (Üçer et al. 2006) and vinyl triazole (Kara 2009) have been used for the removal of heavy metal ions.

Magnetic beads are currently enjoying a fairly ample range of applications in many fields such as physicochemical surface applications (Safarik and Safarikova 2009; Safarik and Safarikova 2010; Schulte and Rode 2006; Şenel et al. 2008; Szablewska et al. 2010; Yavuz et al. 2006). The magnetic character implies that they respond to a magnet, making sampling and collection easier and faster. Magnetic beads are commonly manufactured from polymers since they have a variety of surface functional groups which can be tailored to use in specific applications. Different polymeric magnetic beads are used in the removal of Cr(VI) ions applications (Bayramoğlu and Arica 2008; Demircan et al. 2003; Hu et al. 2005; Huang et al. 2009).

In this study, we have synthesized and characterized the m-poly(DVB-VIM) microbeads. We show that the m-poly(DVB-VIM) microbeads can be used directly for adsorption of Cr(VI) ions from aqueous solutions. In order to clarify the adsorption process, we have conducted kinetic, isothermal and thermodynamic analysis. It was concluded according to the obtained results that the produced m-poly(DVB-VIM) microbeads were useful for the adsorption and repeated use.

2 Experimental

2.1 Materials

Divinylbenzene (DVB) was obtained from Merck (Darmstadt, Germany), and inhibitor was rendered by washing with NaOH solution (3%, w/w) prior to use. 1-Vinyl-imidazole (n-VIM, Aldrich, Steinheim, Germany) was distilled under vacuum (74–76°C, 10 mmHg). 2,2'-Azobisisobutyronitrile (AIBN) was obtained from Merck (Darmstadt, Germany). Poly(vinyl alcohol) (PVAL; Mw: 72,000, 98% hydrolyzed) was supplied by Merck (Darmstadt, Germany). Magnetite nanopowder (Fe₃O₄; diameter 20–30 nm) was obtained from Aldrich (USA). All other reagents were of analytical grade and were used without further purification.

2.2 Synthesis of the m-poly(DVB-VIM) Microbeads

DVB and VIM were copolymerized in suspension by using AIBN and poly(vinyl alcohol) as the initiator and the stabilizer, respectively. Toluene was included in the polymerization recipe as the diluent (as a pore former). A typical preparation procedure is exemplified later in the article. Continuous medium was prepared by dissolving poly(vinyl alcohol) (200 mg) in the purified water (50 ml). For the preparation of

dispersion phase, DVB (2.9 ml; 20 mmol), magnetite Fe₃O₄ nanopowder (0.5 g) and toluene (10 ml) were stirred for 10 min at room temperature. Then, VIM (7.3 ml; 80 mmol) and AIBN (100 mg) were dissolved in the homogeneous organic phase. The organic phase was dispersed in the aqueous medium by stirring the mixture magnetically (500 rpm), in a sealed-cylindrical pyrex polymerization reactor. The reactor content was heated to polymerization temperature (i.e., 65°C) within 4 h, and the polymerization was conducted for 2 h with a 600-rpm stirring rate at 80°C. The final microbeads were extensively washed with ethanol and water to remove any unreacted monomer or diluent and then dried at 50°C in a vacuum oven. The microbeads then were sieved to different sizes. An inspection with a microscope showed that almost all the microbeads were perfectly spherical. Table 1 shows recipe and polymerization conditions for preparation of the m-poly(DVB-VIM) microbeads.

2.3 Characterization Experiments of the m-poly(DVB-VIM) Microbeads

The porosity of the microbeads was measured by a N₂ gas adsorption/desorption isotherm technique (Quantachrome Corporation, Poremaster 60, USA). The specific surface area of beads in a dry state was determined by a multipoint Brunauer–Emmett–Teller

Table 1 The comparison of adsorption capacities of adsorbents Cr(VI)

Sorbents	Capacity (mg g ⁻¹)	References
Peach stone and acrylonitrile-divinylbenzene copolymer based activated carbons	83.00–143.0	Duranoğlu et al. (2010)
Aniline formaldehyde condensate coated silica gel	17.50–65.00	Kumar et al. (2007)
Ethylenediamine-functionalized Fe ₃ O ₄ magnetic polymers		Zhao et al. (2010)
EDA-MPs-2	32.25	
EDA-MPs-4	35.57	
EDA-MPs-6	48.85	
EDA-MPs-8	61.15	
EDA-MPs-10	61.69	
Amino-functionalized macroporous glycidyl methacrylate copolymer		Nastasovic et al. (2009)
SGE-10/12-en	110.1	
SGE-10/16-deta	94.00	
The m-poly(DVB-VIM) microbeads	20.12–81.78 (277 K)	This work
The m-poly(DVB-VIM) microbeads	35.41–101.3 (298 K)	This work
The m-poly(DVB-VIM) microbeads	42.30–110.0 (318 K)	This work
The m-poly(DVB-VIM) microbeads	47.23–115.2 (338 K)	This work

(BET) apparatus (Quantachrome Corporation, Autosorb-6, USA). The porosity and the specific surface area of the microbeads are investigated by the experiments which were given in data terms (Table 2) Pore volumes and average pore diameter for the beads were determined by the BJH (Barrett, Joyner, Halenda) model. The average size and size distribution of the beads were determined by screen analysis performed using standard sieves (Model AS200, Retsch Gmb & Co., KG, Haan, Germany). The surface structures of the beads were visualized and examined by scanning electron microscopy (SEM, CARL ZEISS EVO 40, UK). In order to evaluate the degree of VIM incorporation, the synthesized mesoporous m-poly(DVB-VIM) microbeads were subjected to elemental analysis using a Leco Elemental Analyzer (Model CHNS-932, USA). The magnetization curve of the bead sample was measured by a vibrating sample magnetometer (VSM, Princeton Applied Research, Model 150A, USA). The presence of magnetite nanoparticles in the bead samples was investigated with an electron spin resonance (ESR) spectrophotometer (EL 9, Varian, USA).

2.4 Adsorption Experiments

Batch adsorption experiments were performed by using 0.050 g of the m-poly(DVB-VIM) microbeads with 50 ml of aqueous metal ion solutions in 100-cm³ erlenmeyer flasks, of which concentrations, pH and temperature have already been known. The sample was shaken at 300 rpm in a shaking water bath (Clifton, England). After desired contact time, suspension was filtered. The filtrate was analyzed for metal ions by using an UV-vis spectrophotometer (Shimadzu-2100 UV-vis, Japan).

2.5 Desorption and Repeated Use Experiments

Cr(VI) ions bound to the m-poly(DVB-VIM) microbeads in 1.0 M HNO₃ and 1.0 M NaOH solutions were desorbed in a shaking water bath at 300 rpm for 24 h at room temperature (Clifton, England). The desorption ratio was calculated from the amount of Cr(VI) ions adsorbed on the m-poly(DVB-VIM) microbeads and the final Cr(VI) concentration in the desorption medium, by using the following expression:

$$\text{Desorption ratio} = \frac{\text{Amount of Cr(VI) ions desorbed to the desorption medium}}{\text{Amount of Cr(VI) ions adsorbed on the microbeads}} \times 100. \quad (1)$$

In order to determine the reusability of the magnetic microbeads, consecutive adsorption-desorption cycles were repeated ten times by using the same magnetic microbeads.

3 Results and Discussion

3.1 Characterization of the m-poly(DVB-VIM) Microbeads

The suspension polymerization procedure provided cross-linked the m-poly(DVB-VIM) microbeads in the spherical form of 53–212 μm in diameter. The N₂ adsorption/desorption isotherms for the m-poly(DVB-VIM) and the calculated pore size distributions are plotted in Fig. 1. The BET surface area ($S_{\text{BET}} = 29.47 \text{ m}^2 \text{ g}^{-1}$), the BJH pore size ($D_{\text{BJH}} = 3.761 \text{ nm}$) and pore volume ($V_{\text{p}} = 0.073 \text{ cm}^3 \text{ g}^{-1}$) are calculated (not shown). The sample gave a type IV standard

isotherm with a deep inflection between relative pressure $P/P_0 = 0.4$ and 0.9, characteristic of capillary condensation, indicating the uniformity of the mesopore-size distribution (Duan et al. 2008; Restani et al. 2010; Fu et al. 2007). This indicated that the magnetic beads contained mainly mesopores. The equilibrium swelling ratio for the m-poly(DVB-VIM) microbeads is 44%. It should be also noted that these microbeads are strong enough due to highly cross-linked structure; therefore, they are suitable for column applications. The surface morphology and bulk structures of the m-poly(DVB-VIM) microbeads were visualized by SEM which are presented in Fig. 1. All the beads have a spherical form and rough surface. In the SEM photograph of the bulk structure, a large quantity of well-distributed pores could be observed, and they have a netlike structure. The m-poly(DVB-VIM) microbeads prepared in this study would increase the specific surface area, the binding capacity of microbeads, as well as the mass transfer rate of binding Cr(VI) ions.

Table 2 Kinetic parameters for the adsorption of Cr(VI) ions onto the m-poly(DVB-VIM) microbeads

Parameters	Experimental q_e (mg/g)	Pseudo-first-order kinetic model			Pseudo-second-order kinetic model			Ritch-second order kinetic			Intraparticle diffusion model						
		$k_1 \times 10^{-2}$ (1/min)	q_{eq} (mg/g)	R^2	Δq (%)	h ((mg/g)/min)	$k_2 \times 10^{-3}$ ((g/mg)/min)	q_{eq} (mg/g)	R^2	Δq (%)	$k_R \times 10^{-2}$ (1/min)	q_{eq} (mg/g)	R^2	Δq (%)	k_1 ((mg/g)/min ^{0.5})	R^2	Δq (%)
Temperature (K)																	
277	20.00	1.612	13.26	0.9225	4.952	0.653	1.269	22.68	0.9915	0.7165	1.841	26.39	0.8978	1.7723	1.096	0.7662	6.522
298	34.07	2.695	22.49	0.9567	9.505	2.103	1.477	37.73	0.9903	0.8281	8.001	34.13	0.8919	0.3709	1.631	0.6943	1.264
318	41.99	1.773	16.80	0.8576	12.23	3.509	1.804	44.05	0.9972	0.8677	11.23	40.82	0.9036	0.2694	1.719	0.7152	1.401
338	46.85	1.359	14.71	0.7352	33.00	4.346	1.826	48.78	0.9976	0.8801	12.55	45.87	0.9243	0.2398	1.768	0.6980	1.492

The m-poly(DVB-VIM) microbeads were synthesised by copolymerizing DVB with VIM at a 1:4 molar ratio with Fe₃O₄ in the presence of the initiator AIBN. To evaluate the degree of VIM incorporation into the mesoporous m-poly(DVB-VIM) microbeads, elemental analysis (C%=80.74; H%=7.480; N%=4.230) of the synthesized m-poly(DVB-VIM) microbeads was performed. The incorporation of the VIM was found to be 3.021 mmol/g polymer from the nitrogen stoichiometry.

Magnetic characteristics of magnetic materials are related to their type generally, while those of magnetic materials are usually related to the content of magnetic component inside. Therefore, Fe₃O₄ content is very important to the magnetic responsibility of magnetic materials. In general, the higher Fe₃O₄ content shows the stronger magnetic responsibility (Şenel et al. 2008). For this reason, the average Fe₃O₄ content of the m-poly (DVB-VIM) microbeads was determined by density analysis. The hydrated density of the m-poly(DVB-VIM) microbeads measured at 25°C was 1.41 g/ml. By the same procedure, the density of Fe₃O₄ particles was found to be 4.94 g/ml at 25°C. The density of non-magnetic poly(DVB-VIM) microbeads measured at 25°C was 1.01 g/ml. The magnetic particles volume fraction in the mesoporous m-poly(DVB-VIM) microbeads can be calculated from the following equation derived from the mass balance:

$$\emptyset = (\rho_c - \rho_M) / (\rho_c - \rho_A) \tag{2}$$

where, ρ_A , ρ_c and ρ_M are the densities of non-magnetic poly(DVB-VIM) microbeads, Fe₃O₄ nanopowder, and the m-poly(DVB-VIM) microbeads, respectively. Thus, with the density data mentioned previously, the m-poly (DVB-VIM) microbeads gel volume fraction in the magnetic beads was estimated to be 89.2%. Therefore, the average Fe₃O₄ content of the resulting m-poly (DVB-VIM) microbeads was 10.2%. The presence of magnetite nanopowder in the polymer structure was also confirmed by the ESR (not shown). A peak of magnetite was detected in the ESR spectrum. It should be noted that the non-magnetic beads cannot be magnetized under this condition. It reflects response ability of magnetic materials to the change of external magnetic field firstly, and it characterizes the ability of magnetic materials to keep magnetic field strength when the external magnetic field is removed. In order to show the magnetic stability, the m-poly(DVB-VIM) microbeads were kept in distilled water and ambient air for 3 months, and

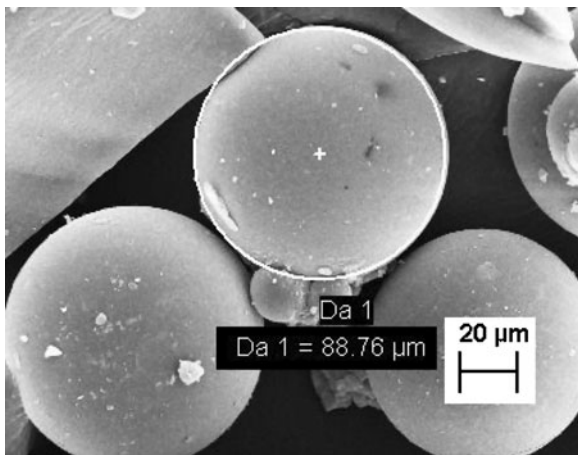


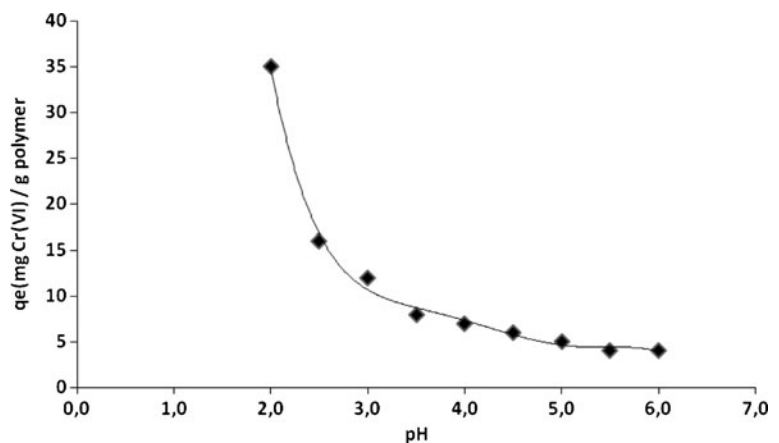
Fig. 1 SEM photograph of the m-poly(DVB-VIM) microbeads

the same ESR spectrum was obtained. With the goal of testing the mechanical stability of the m-poly(DVB-VIM) microbeads, a bead sample was treated in a ball mill for 12 h. SEM photographs show that a zero percentage of the sample was broken. The g factor given in Fig. 3 can be considered as quantity characteristic of the molecules in which the unpaired electrons are located, and it is calculated from Eq. 3. The measurement of the g factor for an unknown signal can be a valuable aid in the identification of a signal. In the literature, the g factor for Fe^{+3} is determined between 1.4 and 3.1 for low spin, and 2.0 and 9.7 for high spin complexes [30]. The g factor was found to be 2.44 for the m-poly(DVB-VIM) microbeads structure.

$$g = h \cdot \vartheta / \beta \cdot H_r \quad (3)$$

Here, h is the Planck constant (6.626×10^{-27} erg s^{-1}); β is Universal constant (9.274×10^{-21} erg G^{-1}); ϑ is

Fig. 2 Effect of pH on adsorption of Cr(VI) ions of the m-poly(DVB-VIM) microbeads



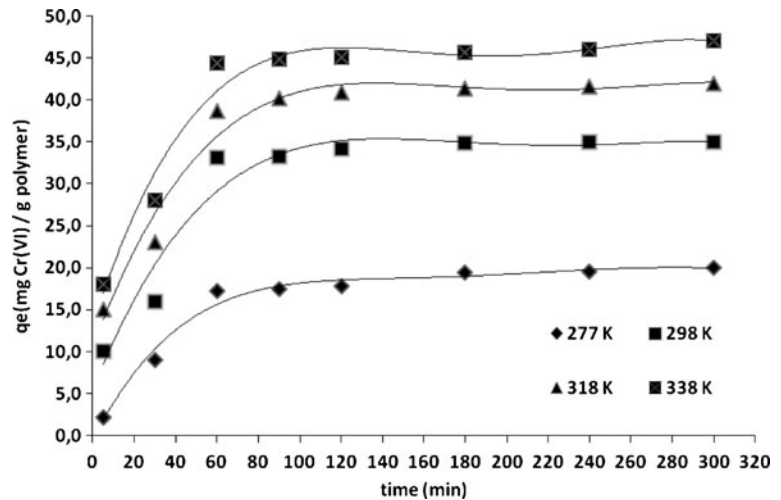
frequency (9.707×10^9 Hz) and H_r is resonance of magnetic field (G).

3.2 Adsorption of Cr(VI) Ions from Aqueous Solutions

3.2.1 Effect of pH on Adsorption of Cr(VI) Ions

The adsorption of the metal ions onto an adsorbent varies generally with pH because pH causes to change the radius of hydrolyzed cation and the charge of the adsorbent surface. Therefore, in this study, the adsorption of Cr(VI) ions onto the m-poly(DVB-VIM) microbeads is studied as a function of pH. The initial pH values of Cr(VI) solutions were kept between 2.0 and 6.0. The relationship between initial pH and the amounts of Cr(VI) adsorbed on the m-poly(DVB-VIM) microbeads for the initial solution concentration of 100 mg dm^{-3} at 25°C and a contact time of 300 min is illustrated in Fig. 2. When initial pH values of Cr(VI) solutions are increased from 2.0 to 6.0, the amounts of Cr(VI) adsorbed per unit mass of adsorbent are decreased. For example, the amounts of Cr(VI) ions adsorbed per unit adsorbent decrease from 35.21 to 4.55 mg g^{-1} for Cr(VI) ions when the pH value increases from 2.0 to 6.0. As seen in Fig. 4, pH 2 is a value for the maximum adsorption of Cr(VI) ions. The adsorption of Cr(VI) ions depends on the protonation or unprotonation of functional groups on the surface of the microbeads. Cr(VI) ions exist in anionic forms (i.e. $\text{Cr}_2\text{O}_7^{2-}$, HCrO_4^- , CrO_4^{2-} and HCr_2O_7^-) in aqueous medium, and fraction of any particular species is dependent on chromium concentration and pH [15]. At acidic pH, the imidazole groups of the m-poly(DVB-VIM) microbeads are positively charged, which leads to an electrostatic attraction for the negatively

Fig. 3 Effect of temperature on adsorption of Cr(VI) ions of the m-poly(DVB-VIM) microbeads



charged chromium species. The fact that a rise in the pH causes the decrease of the adsorption of metal ions is attributed to that protonation of imidazole groups on the m-poly(DVB-VIM) microbeads has become more positive.

3.2.2 Effect of Temperature on Adsorption of Cr(VI) Ions

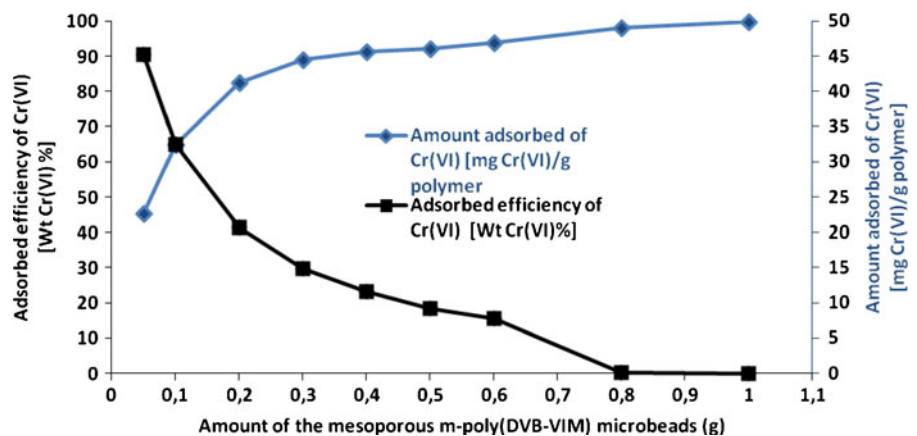
The uptake Cr(VI) ions (mg g^{-1}) were increased from 20.11 to 47.36 mg g^{-1} with the rise in temperature from 4 to 65°C (Fig. 3). Equilibrium time was found to be 300 min indicating that the equilibrium time was independent of temperature. These results also showed that the adsorption was endothermic in nature. The imidazole groups of the m-poly(DVB-VIM) microbeads are partially protonated at all temperatures, but their deprotonation degree decreases at higher temperatures

resulting in a slight increase in the capacities of Cr(VI) ions at high temperature. Where only adsorption of Cr(VI) ions is involved, the temperature effect on retention time is relatively small. Empirical studies show that temperature has a small effect on adsorption (Moussavi and Barikbin 2010; Liu et al. 2010; Rao and Rehman 2010; Hena 2010; Mustafa et al. 2010; Wang et al. 2010; Chowdhury et al. 2010; Sharma et al. 2009).

3.2.3 Effect of Adsorbent Dosage on Adsorption of Cr(VI) Ions

The effect of adsorbent dosage on the adsorption of Cr(VI) ions is shown in Fig. 4. The percentage removal increases from 45.2 to 99.9% by increasing the adsorbent dosage from 50 to 1000 mg. It is apparent from Fig. 4 that by increasing the resin amount, the

Fig. 4 Effect of adsorbent dosage on adsorption of Cr(VI) ions



adsorption efficiency increases, but adsorption density, the amount adsorbed per unit mass, decreases. It is readily understood that the number of available adsorption sites increases by increasing the adsorbent amount, but the drop in adsorption capacity is basically due to the sites remaining unsaturated during the adsorption process (Unnithan et al. 2004; Göde and Pehlivan 2005; Jain et al. 2010; Göde et al. 2010; Kumar et al. 2008).

3.2.4 Effect of Initial Concentration of Cr(VI) Ions on Adsorption of Cr(VI) Ions

Eleven different concentrations for Cr(VI) ions, i.e. concentrations of 100, 200, 300, 400, 500, 600, 700, 800, 1000, 1500 and 2000 mg dm^{-3} , are selected to investigate the effect of initial concentration of Cr(VI) ions onto the m-poly(DVB-VIM) microbeads, and the amounts of Cr(VI) ions adsorbed at equilibrium at 293, 303, 318 and 333 K, respectively, and pH 2 are graphed in Fig. 5. As shown in Fig. 5, with increasing initial concentration of Cr(VI) ions from 100 to 2000 mg dm^{-3} , the amount of Cr(VI) ions adsorbed by adsorbent increases from 20.04 to 81.11, from 35.45 to 101.7, from 41.93 to 110.2 and from 46.95 to 115.3 mg g^{-1} of polymer at 293, 303, 318 and 333 K, respectively.

The adsorption capacities of the m-poly(DVB-VIM) microbeads obtained with Cr(VI) ions are comparable to values reported in the previous studies. Table 1 presents the comparison of adsorbent capacity (milligrams per gram) of various adsorbents reported in the literature [Duranoğlu et al. 2010; Kumar et al. 2007; Nastasovic et al. 2009;

Zhao et al. 2010]. The comparison of the adsorption capacities of the m-poly(DVB-VIM) microbeads used in this work with those reported in the previous work shows that the adsorbent is suitable for this purpose.

3.3 Analysis of Adsorption of Cr(VI) Ions from Aqueous Solutions

3.3.1 Analysis of Adsorption Kinetics

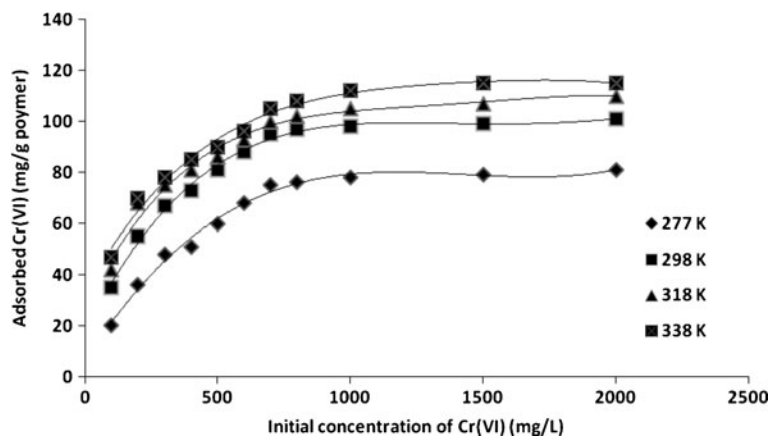
Numerous adsorption processes have been investigated particularly during the past 25 years. It has been known that adsorption processes could be dependent on and controlled by different kinds of mechanisms such as diffusion control, mass transfer, chemical reactions and particle diffusion. The pseudo-first-order kinetic model, pseudo-second-order kinetic model, modified Ritchie's-second-order kinetic model and intraparticle diffusion model were used for testing dynamic experimental data at the initial concentration, 100 mg/L , of Cr(VI) ions and four temperatures (277, 298, 318 and 338 K) in pH 2.0.

The pseudo-first-order kinetic model of Lagergren is given as follows (Lagergren 1898):

$$\log(q_e - q_t) = \log q_e - k_1 t / 2.303 \quad (4)$$

where q_e and q_t (milligrams per gram) are the amounts of the Cr(VI) ions adsorbed at equilibrium and at time (min), respectively. k_1 (1/min) is the rate constant of pseudo-first-order adsorption, and q_e is the adsorption capacity at equilibrium.

Fig. 5 Effect of initial concentration of Cr(VI) ions onto the m-poly(DVB-VIM) microbeads at various temperatures



The pseudo-second-order kinetic model can be expressed as (Ho and McKay 1999) follows:

$$\frac{t}{q_t} = \frac{1}{k_2 q_e^2} + \frac{1}{q_e} t \tag{5}$$

where q_e and q_t (milligrams per gram) have the same definitions as in Eq. 4, and k_2 is the pseudo-second-order rate constant at equilibrium (grams per milligram per minute). The initial adsorbent rate h (milligrams per gram per minute) can be determined from k_2 and q_e values using the following equation:

$$h = k_2 q_e^2. \tag{6}$$

The modified Ritchie’s-second-order kinetic model (Ritchie 1977) is expressed as:

$$\frac{1}{q_t} = \frac{1}{k_R q_e t} + \frac{1}{q_e} \tag{7}$$

where q_t and q_e (milligrams per gram) have the same definitions as in Eq. 4, and k_R is the rate constant (1/min) of the modified Ritchie’s-second-order kinetic model.

The intraparticle diffusion model can be described as (Osman et al. 2011):

$$q_t = k_i t^{1/2} \tag{8}$$

where q_t (milligrams per gram) has the same definition as in Eq. 5, and k_i is the intraparticle diffusion rate constant (milligrams per gram per $^{1/2}$ minute).

To quantitatively compare the applicability of each model, a normalized standard deviation (Δq) is calculated as follows:

$$\Delta q(\%) = 100 \times \sqrt{\frac{\sum \left[\frac{q_{e,exp} - q_{e,cal}}{q_{e,exp}} \right]^2}{n - 1}}. \tag{9}$$

where n is the number of data points and q_e is the adsorbent capacity at the equilibrium experimental conditions ($q_{e,exp}$) and calculated ($q_{e,cal}$) respectively. Since Δq represents agreement between the experimental and the predicted data points, it provides a numerical measure to interpret the goodness of fit of a given mathematical model to the data (Zolgharnein and Shahmoradi 2010; Wu et al. 2001).

The validity of the order of adsorption process is based on three criteria: the first one is the regression coefficients, the second is predicted q_e values, and the third is the normalized standard deviation (Daoud et

al. 2010). The validities of these four kinetic models for all temperatures are checked and depicted in Fig. 6a–d. The values of the parameters, correlation coefficient and normalized standard deviation obtained from these four kinetic models are all listed in Table 2. Among these figures, Fig. 6b shows a good agreement pseudo-second-order kinetic model. As shown in Table 2, the values of R^2 for pseudo-second-order kinetic model are extremely high (all greater than 0.99), and the values of Δq (%) for pseudo-second-order kinetic model are low (all less than 0.88), followed by those of the modified Ritchie’s-second-order kinetic model (all greater than 0.89 for R ; all less than 1.77 for Δq (%)) (Fig. 6c), intraparticle diffusion model (all greater than 0.69 for R ; all less than 6.52 for Δq (%)) (Fig. 6d) and pseudo-first-order kinetic model (all greater than 0.73 for R ; all less than 33.00 for Δq (%)) (Fig. 6a), respectively. Meanwhile, the calculated q_e values estimated from pseudo-first-order kinetic model are different from the experimental ones (q_e) (see Table 2). The calculated q_e values obtained from modified Ritchie’s-second-order plots are found to agree perfectly with the experimental q_e values. The calculated q_e values estimated from pseudo-second-order kinetic model agree slightly with the experimental q_e values, and then, because of mass transfer effects, the intraparticle diffusion model was obtained for all temperatures. The plots for intraparticle diffusion model are demonstrated in Fig. 6d. The intraparticle diffusion of Cr(VI) ions within the particles of the m-poly(DVB-VIM) microbeads used as an adsorbent was found to be rate controlling in the adsorbent process. Consequently, the adsorption process could be best described both by the pseudo-second-order kinetic model and by the modified Ritchie’s-second-order kinetic model. This also implies that the rate-limiting step may be the chemical adsorption (Plazinski et al. 2009; Zhao et al. 2010).

The values of the pseudo-second-order rate constant, k_2 , were found to increase from 1.269×10^{-3} to 1.826×10^{-3} g/mg/min, for an increase in the solution temperature of 277 to 338 K. There is a linear relationship between k_2 and temperature (Fig. 7). The adsorption rate constant is usually expressed as a function of solution temperature by the following Arrhenius type relationship (Hoa and Ofomaja 2006):

$$\ln k_2 = \ln k_0 - \frac{E_a}{RT} \tag{10}$$

Fig. 6 Adsorption kinetics of adsorption of Cr(VI) ions by the mesoporous m-poly (DVB-VIM) microbeads at different temperatures.

- a** Pseudo-first-order.
- b** Pseudo-second-order.
- c** Ritchie's-second-order.
- d** Intraparticle diffusion

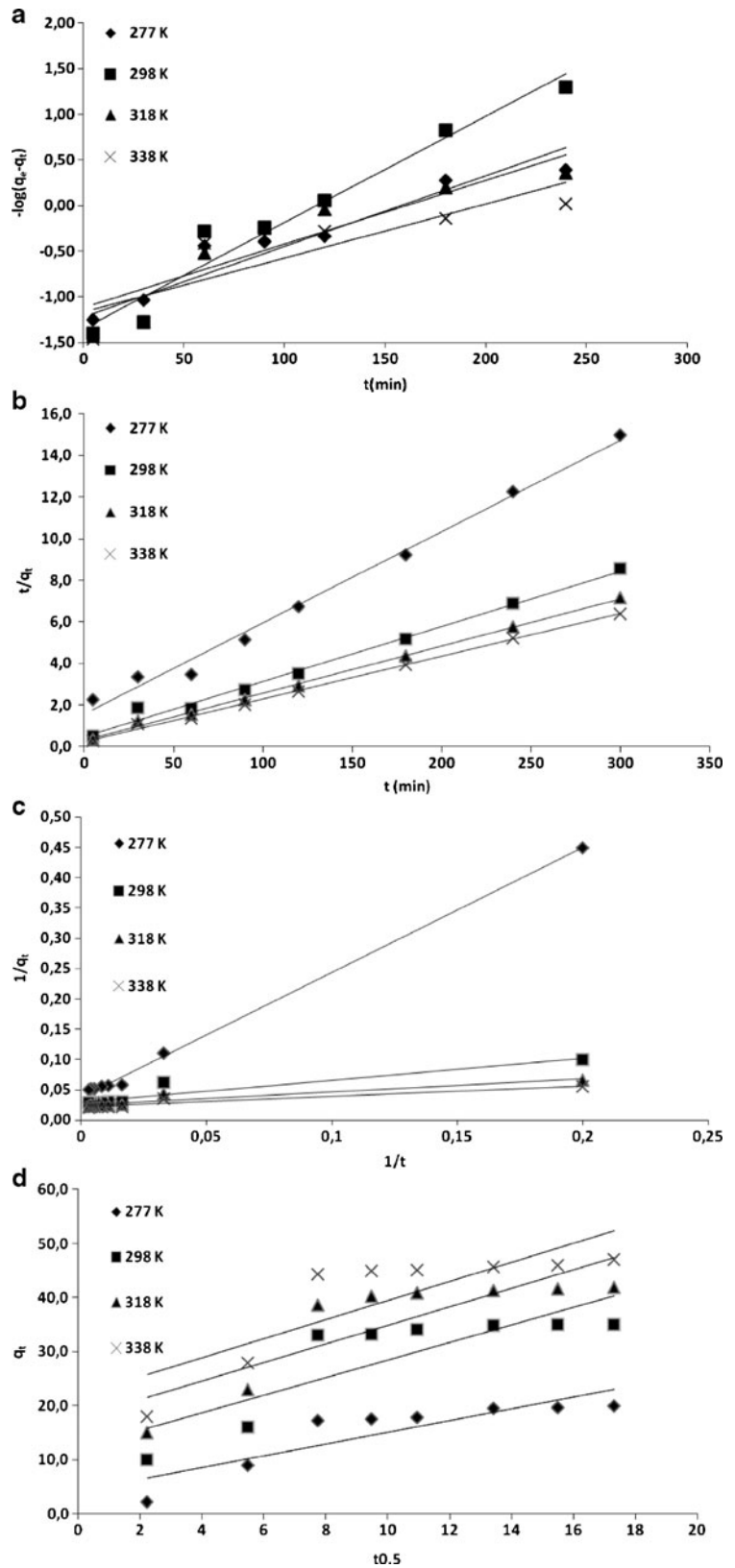
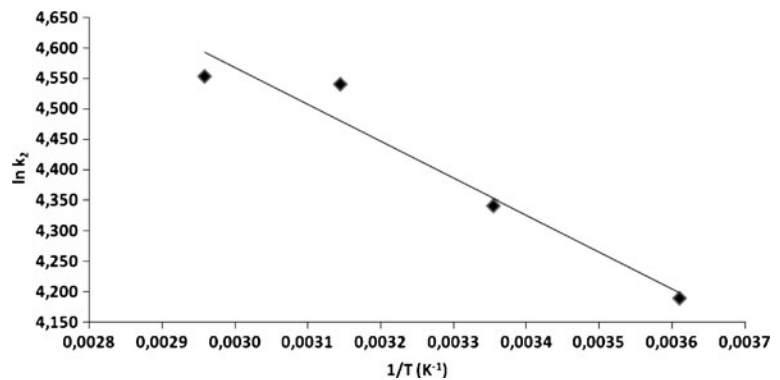


Fig. 7 Arrhenius plot



where k_2 is the rate constant of pseudo-second-order of adsorption (grams per milligram per minute), k_0 is the independent temperature factor (grams per milligram per minute), R is the gas constant ($8.314 \text{ J mol}^{-1} \text{ K}^{-1}$), and T is the solution temperature (Kelvin).

Therefore, the relationship between k_2 and T can be represented in an Arrhenius form as:

$$\ln k_2 = 6.3807 - \left(\frac{604.35}{T} \right). \quad (11)$$

From this equation, the rate constant for adsorption, k_0 , is $5.90 \times 10^2 \text{ g/mg/min}$, and the activation energy for adsorption, E_a , is 5.024 kJ/mol . The magnitude of activation energy explains the type of sorption. Two main types of adsorption can occur, physical or chemical. In physical adsorption, the equilibrium is usually attained rapidly and easily reversible, because the energy requirements are small. The activation energy for physical adsorption is usually not more than $4.184 \text{ kJ mol}^{-1}$ ($1.0 \text{ kcal mol}^{-1}$), because the forces involved in physical adsorption are weak. Chemical adsorption is specific and involves forces much stronger than physical adsorption. Two kinds of chemisorption are encountered: activated and, less frequently, nonactivated. Activated chemical adsorption means that the rate varies with temperature according to a finite activation energy in the Arrhenius equation (high E_a). However, in some systems chemical adsorption occurs very rapidly, suggesting the activation energy is near zero. This is termed nonactivated chemical adsorption. It is difficult to decide which mechanism is effective in the adsorption of Cr(VI) ions on m-poly(DVB-VIM) microbeads, only taking activation energies into consideration. As the observed value of the activation energy of adsorption of Cr(VI) ions on m-poly(DVB-VIM) microbeads is greater for less

than 4.184, the adsorption process may involve both physical and chemical adsorption (Ertugay and Bayhan 2010; Sağ and Kutsal 2000).

3.4 Analysis of Adsorption Isotherm

The relationship between the amount of Cr(VI) ions adsorbed onto the adsorbent surface and the remaining Cr(VI) ions concentration in the aqueous phase at equilibrium can be observed by the adsorption equilibrium isotherm analysis as shown in the investigation of the effect of initial concentration of Cr(VI) ions. This relationship showed that the adsorption capacity increased with the equilibrium concentration of the Cr(VI) ions in solution, progressively reaching saturation of the adsorbent. Adsorption isotherm curves indicate that adsorption phenomenon may be represented by isotherms of type I which represent a monolayer adsorption until the saturation of active sites. The adsorption isotherms were investigated using three equilibrium models, which are the Langmuir, Freundlich and Dubinin–Radushkevich (D–R) isotherm models. To quantitatively compare the applicability of each model, a normalized standard deviation (Δq) is calculated as in Eq. 9.

Freundlich adsorption isotherm is given as (Kara et al. 2006):

$$q_e = K_f C_e^{1/n}. \quad (12)$$

In logarithmic form,

$$\ln q_e = \ln K_f + \frac{1}{n} \ln C_e \text{ (linear form)} \quad (13)$$

where q_e is the amount of metal ions adsorbed at equilibrium time (milligrams per gram), and C_e is the equilibrium concentration of the metal ions in solution

Table 3 Parameters of Langmuir, Freundlich and Dubinin–Raduskevich isotherm models, for the adsorption of Cr(VI) ions onto the m-poly(DVB-VIM) microbeads

Parameters	Langmuir isotherm constants			Freundlich isotherm constants			Dubinin–Raduskevich isotherm constants							
	$K_L \times 10^{-3}$ (L/mg)	Q_L (mg/g)	R^2 (%)	Δq	R_L	K_F (mg/g) (L/mg) ^{1/n}	n	R^2	Δq (%)	Q_{D-R} (mg/g)	$K_{D-R} \times 10^{-9}$ (mol ² /J ²)	E (kJ/mol)	R^2	Δq (%)
277	4.353	92.59	0.9916	0.7066	0.6967–0.0711	3.899	2.302	0.8761	0.9517	164.6	-8.745	7.561	0.9363	0.1677
298	7.731	108.7	0.9979	0.7944	0.5640–0.0794	11.46	3.198	0.8880	0.1379	167.1	-5.307	9.701	0.9488	0.0926
318	8.599	116.3	0.9986	0.8005	0.5377–0.0720	17.38	3.801	0.8903	0.1082	162.3	-3.845	11.40	0.9551	1.3510
338	8.664	123.5	0.9981	0.8006	0.5388–0.0715	19.44	3.956	0.9347	0.0997	166.2	-3.223	12.45	0.9743	1.4878

(milligrams per liter). K_f (mg/g)(L/mg)^{1/n} and n are isotherm constants which indicate capacity and intensity of the adsorption, respectively.

Freundlich [0.88<R² and 0.95> Δq (%)] and D–R isotherms [0.94<R² and 1.48> Δq (%)] are not as adequate as Langmuir model [0.99<R² and 0.80> Δq (%)]. The values of K_f and n were calculated from the slope and intercept of the plot $\ln q_e$ versus $\ln C_e$ (not shown). The value of K_f and n obtained are shown in Table 3. As shown in Table 3, the value of n ranges between 3.956 and 2.302. If the value of n is in the range 1< n <10, the adsorption is favorable [65].

The Langmuir isotherm is expressed as (Tekin et al. 2006):

$$\frac{C_e}{q_e} = \frac{1}{Q_L K_L} + \frac{C_e}{Q_L} \tag{14}$$

where Q_L (milligrams per gram) is the maximum amount of Cr(VI) per unit weight of the m-poly (DVB-VIM) microbeads to form complete monolayer coverage on the surface bound at high equilibrium Cr (VI) concentration C_e , and K_L is Langmuir constant related to the affinity of binding sites (liters per milligram). Q_L represents a particle limiting adsorption capacity when the surface is fully covered with Cr (VI) and assists in the comparison of adsorption performance. Q_L and K_L are calculated from the slopes and intercepts of the straight lines of the plot of $\frac{C_e}{q_e}$ versus C_e (not shown).

Parameters of the Langmuir and Freundlich isotherms are computed in Table 3. Langmuir isotherm fits quite well with the experimental data correlation coefficient, whereas the low correlation coefficients show poor agreement of the Freundlich isotherm with the experimental data. Calculated maximum capacities are close to maximum capacities obtained at equilibrium (Table 3). The fact that the Langmuir isotherm

Table 4 ΔG^0 values for the different solution temperatures used for Cr(VI) ions removal with the m-poly(DVB-VIM) microbeads

Solution temperature (K)	ΔG^0 (kJ/mol)
277	-12.49
298	-14.86
318	-16.14
338	-17.17

Table 5 ΔH^0 and ΔS^0 for the solution temperatures used for Cr (VI) ions removal with the m-poly(DVB-VIM) microbeads

ΔH^0 (kJ/mol)	ΔS^0 (J/mol K)
8.655	77.40

fits the experimental data very well may be due to homogenous distribution of active sites on the m-poly (DVB-VIM) microbeads surface, since the Langmuir equation assumes that the surface is homogeneous (Doğan et al. 2000).

Furthermore, the essential characteristic of the Langmuir isotherm can be expressed by a dimensionless separation factor called equilibrium parameter R_L (Namasivayam and Kavita 2002).

$$R_L = \frac{1}{1 + KC_e} \tag{15}$$

where K is the Langmuir constant (cubic decimeters per milligram) and C_e is the initial metal ion concentration (milligrams per cubic decimeter).

Parameter R_L indicates the shape of isotherm as follows:

Value of R_L	Type of isotherm
$R_L > 1$	Unfavorable
$R_L = 1$	Linear
$0 < R_L < 1$	Favorable
$R_L = 0$	Irreversible

R_L value between 0 and 1 indicates a favorable adsorption. Herein, the values of R_L between 0 and 1 indicate a favorable adsorption. Here, R_L values obtained are listed in Table 3. The fact that all the R_L values for the adsorption of Cr(VI) ions onto the m-

poly(DVB-VIM) microbeads are in the range 0.5388–0.6967 shows that the adsorption process is favorable.

Although the Langmuir and Freundlich isotherm models are widely used, they do not give information on the adsorption mechanism. To this aim, the equilibrium data were tested with the Dubinin–Radushkevich isotherm model (D–R isotherm). This isotherm model predicts the nature of the adsorbate sorption onto the adsorbent, and it is used to calculate the mean free energy of adsorption. The non-linear D–R isotherm is expressed as:

$$Q_e = Q_{D-R} \exp(-K_{D-R} \varepsilon^2) \tag{16}$$

and the linearized form of the equation is given as:

$$\ln Q_e = \ln Q_{D-R} - K_{D-R} \varepsilon^2 \tag{17}$$

where Q_e is the amount of solute adsorbed per mass of adsorbent (milligrams per gram), Q_{D-R} is the maximum adsorption capacity (milligrams per gram), K_{D-R} is the D–R constant (square moles per square Joule) and ε is the Polanyi potential (Joules per mole), which can be calculated as:

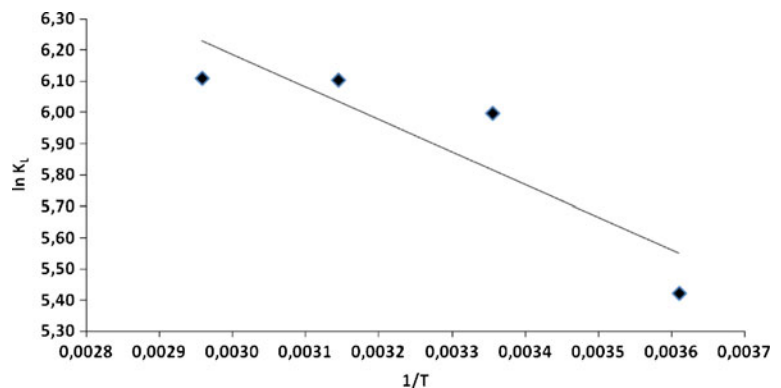
$$\varepsilon = RT(\ln 1 + 1/C_e) \tag{18}$$

where R is the gas constant (Joules per mole Kelvin), T the absolute temperature (Kelvin) and C_e the equilibrium concentration of the adsorbate in aqueous solution (milligrams per liter) (Laus et al. 2010; Chen et al. 2008; Tripathy and Raichur 2008). The values of Q_{D-R} and K_{D-R} were calculated and are shown in Table 3.

The mean free energy of adsorption (E_{fe}) was calculated from the K_{D-R} values using the equation:

$$E_{fe} = 1/\sqrt{-2K_{D-R}} \tag{19}$$

Fig. 8 The plot of $\ln K_L$ versus $1/T$ for the determination of thermodynamic parameters for adsorption of Cr(VI) ions on the m-poly (DVB-VIM) microbeads



The E_{fc} value is used to ascertain the type of adsorption process under consideration. If this value is between 8 and 16 kJ mol⁻¹, the adsorption process can be assumed to involve chemical sorption. On the other hand, values lower than 8 kJ mol⁻¹ indicate that the adsorption process is of a physical nature (Özcan et al. 2005; Ünlü and Ersoz 2006; Tassist et al. 2010). In this study, D–R isotherm model is in the range 0.9366–0.9743, and the E values obtained using the D–R constant, in the non-linear form, were 7.561 kJ mol⁻¹ for 277 K, 9.701 kJ mol⁻¹ for 298 K, 11.40 kJ mol⁻¹ for 318 K and 12.45 kJ mol⁻¹ for 338 K, indicating that the adsorption of Cr(VI) ions onto the m-poly(DVB-VIM) occurs via a chemical process for all the temperatures.

3.5 Analysis of Adsorption Thermodynamic

Temperature dependence of equilibrium constant, K_L , can be used to determine the thermodynamic parameters [75]. The van't Hoff equation is used to evaluate the variation of equilibrium constant with temperature. The integrated form of this equation is given as:

$$\ln K_L = \frac{\Delta S^0}{R} - \frac{\Delta H^0}{R} \left(\frac{1}{T} \right). \quad (20)$$

The enthalpy (ΔH^0) and entropy (ΔS^0) changes of the process can be determined from the slope and intercept of a line obtained by plotting $\ln K_L$ versus $1/T$. The equation free energy for each temperature is then obtained as:

$$\Delta G^0 = \Delta H^0 - T \Delta S^0. \quad (21)$$

From Eq. 20, Gibbs free energy change of adsorption (ΔG^0) was calculated as -12.49, -14.86, -16.14 and -17.17 kJ/mol⁻¹ for the adsorption of Cr(VI) ions onto the m-poly(DVB-VIM) microbeads at 277, 298, 318 and 338 K, respectively (Table 4). The negative ΔG^0 values indicated that the adsorption of Cr(VI) ions onto the m-poly(DVB-VIM) microbeads was thermodynamically feasible and spontaneous. The enthalpy (ΔH^0) and entropy (ΔS^0) changes were determined as 8.655 kJ/mol and 77.40 J/molK, respectively (Table 5), from $\ln K_L$ versus $1/T$ plot (Fig. 8). The positive value of ΔH^0 confirmed the endothermic character of the adsorption process. The positive values of ΔS^0 also revealed the increase of randomness at the solid-solute interface during the adsorption of Cr

(VI) ions onto the m-poly(DVB-VIM) microbeads. The low value of ΔS^0 indicated that no remarkable change on entropy occurs.

3.6 Desorption and Repeated Use

The use of an adsorbent in the adsorption process depends not only on the adsorptive capacity, but also on how well the adsorbent can be regenerated and used again. For repeated use of an adsorbent, adsorbed metal ions should be easily desorbed under suitable conditions. Desorption of the adsorbed Cr(VI) ions from the m-poly(DVB-VIM) microbeads was also studied in a batch experimental system. Desorption experiments put into evidence that after 2 h contact NaOH solutions (1.0 mol/L, desorption percentage 97%) were more efficient than HCl solutions (1.0 mol/L, desorption percentage 33%) to desorb Cr(VI) ions for the adsorbent. The repeated use for NaOH solutions of the m-poly(DVB-VIM) microbeads shows that the adsorption–desorption process is a reversible process. Five cycles of adsorption–desorption experiments were conducted to examine the capability of the mesoporous m-poly(DVB-VIM) microbeads to retain Cr(VI) ions removal capacity. The adsorption capacity of the m-poly(DVB-VIM) microbeads was decreased only 4% during a ten-adsorption–desorption cycle.

Acknowledgment This work was supported by the Research Foundation of Uludag University (Project No: UAP(F)-2011/35).

Open Access This article is distributed under the terms of the Creative Commons Attribution Noncommercial License which permits any noncommercial use, distribution, and reproduction in any medium, provided the original author(s) and source are credited.

References

- Bayramoglu, G., & Arica, M. Y. (2008). Adsorption of Cr(VI) onto PEI immobilized acrylate-based magnetic beads: isotherms, kinetics and thermodynamics study. *Chemical Engineering Journal*, 139, 20–28.
- Bayramoğlu, G., & Arica, M. Y. (2005). Ethylenediamine grafted poly(glycidylmethacrylate-co-methylmethacrylate) adsorbent for removal of chromate anions. *Separation and Purification Technology*, 45, 192–199.
- Chen, A. H., Liu, S. C., & Chen, C. Y. (2008). Comparative adsorption of Cu(II), Zn(II), and Pb(II) ions in aqueous solution on the crosslinked chitosan with epichlorohydrin. *Journal of Hazardous Materials*, 154, 184–191.

- Chowdhury, P., Mondal, P., & Roy, K. (2010). Synthesis of cross-linked graft copolymer from [2-(methacryloyloxy ethyl) trimethylammonium chloride and poly(vinyl alcohol) for removing chromium(VI) from aqueous solution. *Polymer Bulletin*, *64*, 351–362.
- Copello, G. J., Varela, F., Vivot, R. M., & Diaz, L. E. (2008). Immobilized chitosan as biosorbent for the removal of Cd (II), Cr(III) and Cr(VI) from aqueous solutions. *Bioresource Technology*, *99*, 6538–6544.
- Daoud, F. B., Kaddour, S., & Sadoun, T. (2010). Adsorption of cellulase *Aspergillus niger* on a commercial activated carbon: kinetics and equilibrium studies. *Colloids and Surfaces. B, Biointerfaces*, *75*, 93–99.
- Demircan, Z., Tekol, E., Tanyolaç, D., & Özdural, A. R. (2003). Para-magnetic polyvinylbutyral particles containing activated carbon as a new adsorbent. *Chemical Engineering Communications*, *190*, 831–842.
- Doğan, M., Alkan, M., & Onganer, Y. (2000). Adsorption of methylene blue from aqueous solution onto perlite. *Water, Air, and Soil Pollution*, *120*, 229–248.
- Duan, G., Zhang, C., Li, A., Yang, X., Lu, L., & Wang, X. (2008). Preparation and characterization of mesoporous zirconia made by using a poly(methyl methacrylate) template. *Nanoscale Research Letters*, *3*, 118–122.
- Duran, A., Soylak, M., & Tuncel, S. A. (2008). Poly(vinyl pyridine-poly ethylene glycol methacrylate-ethylene glycol dimethacrylate) beads for heavy metal removal. *Journal of Hazardous Materials*, *155*, 114–120.
- Duranoğlu, D., Trochimczuk, A. W., & Beker, Ü. (2010). A comparison study of peach stone and acrylonitrile-divinylbenzene copolymer based activated carbons as chromium(VI) sorbents. *Chemical Engineering Journal*, *165*, 56–63.
- Ebraheem, K. A. K., & Hamdi, S. T. (1997). Synthesis and properties of a copper selective chelating resin containing a salicylaldehyde group. *Reactive and Functional Polymer*, *34*, 5–10.
- Ertugay, N., & Bayhan, Y. K. (2010). The removal of copper (II) ion by using mushroom biomass (*Agaricus bisporus*) and kinetic modelling. *Desalination*, *255*, 137–142.
- Fiol, N., Escudero, C., & Villaescusa, I. (2008). Chromium sorption and Cr(VI) reduction to Cr(III) by grape stalks and yohimbe bark. *Bioresource Technology*, *99*, 5030–5036.
- Fontanals, N., Marce, R. M., Galia, M., & Boorrull, F. (2004). Synthesis of hydrophilic sorbents from *N*-vinylimidazole/divinylbenzene and the evaluation of their sorption properties in the solid-phase extraction of polar compounds. *Journal of Macromolecular Science Pure & Applied Chemistry*, *A42*, 2019–2025.
- Fu, L. J., Zhang, T., Cao, Q., Zhang, H. P., & Wu, Y. P. (2007). Preparation and characterization of three-dimensionally ordered mesoporous titania microparticles as anode material for thium ion battery. *Electrochemistry Communications*, *9*, 2140–2144.
- Göde, F., & Pehlivan, E. (2005). Removal of Cr(VI) from aqueous solution by two Lewatit-anion exchange resins. *Journal of Hazardous Materials*, *B119*, 175–182.
- Göde, F., Öztürk, N., Sert, Y., & Bahçeli, S. (2010). Adsorption of Cr(VI) from aqueous solutions onto raw and acid-activated Reşadiye and Hançılı clays. *Spectroscopy Letters*, *43*, 68–78.
- Hena, S. (2010). Removal of chromium hexavalent ion from aqueous solutions using biopolymer chitosan coated with poly 3-methyl thiophene polymer. *Journal of Hazardous Materials*, *181*, 474–479.
- Ho, Y. S., & McKay, G. (1999). Pseudo-second-order model for sorption processes. *Process Biochemistry*, *34*, 451–465.
- Hoa, Y.-S., & Ofomaja, A. E. (2006). Kinetic studies of copper ion adsorption on palm kernel fibre. *Journal of Hazardous Materials*, *B137*, 1796–1802.
- Hu, J., Chen, G. H., & Irene, M. C. L. (2005). Removal and recovery of Cr(VI) from wastewater by maghemite nanoparticles. *Water Research*, *39*, 4528–4536.
- Huang, G., Zhang, H., Shi, J. X., & Langrish, T. A. G. (2009). Adsorption of chromium(VI) from aqueous solutions using cross-linked magnetic chitosan beads. *Industrial and Engineering Chemistry Research*, *48*, 2646–2651.
- Jain, M., Garg, V. K., & Kadirvelu, K. (2010). Adsorption of hexavalent chromium from aqueous medium onto carbonaceous adsorbents prepared from waste biomass. *Journal of Environmental Management*, *91*, 949–957.
- Kantipuly, C., Katragadda, S., Chow, A., & Gesser, H. D. (1990). Chelating polymers and related supports for separation and preconcentration of trace-metals. *Talanta*, *37*, 491–517.
- Kara, A. (2009). Adsorption of Cr(VI) ions onto poly(ethylene glycol dimethacrylate-1-vinyl-1,2,4-triazole). *Journal of Applied Polymer Science*, *114*, 948–955.
- Kara, A., Uzun, L., Beşirli, N., & Denizli, A. (2004). Poly(ethylene glycol dimethacrylate-*n*-vinyl imidazole) beads for heavy metal removal. *Journal of Hazardous Materials*, *106B*, 93–99.
- Kara, A., Acemioğlu, B., Alma, M. H., & Cebe, M. (2006). Adsorption of Cr(III), Ni(II), Zn(II), Co(II) ions onto phenolated wood resin. *Journal of Applied Polymer Science*, *101*, 2838–2846.
- Kumar, P. A., Ray, M., & Chakraborty, S. (2007). Hexavalent chromium removal from wastewater using aniline formaldehyde condensate coated silica gel. *Journal of Hazardous Materials*, *113*, 24–32.
- Kumar, P. A., Chakraborty, S., & Ray, M. (2008). Removal and recovery of chromium from wastewater using short chain polyaniline synthesized on jute fiber. *Chemical Engineering Journal*, *141*, 130–140.
- Lagergren, S. (1898). Zur theorie der sogenannten Adsorption gel oster stoffe. *Kungliga Svenska Vetenskapsakademiens Handlingar*, *25*(4), 1–39.
- Laus, R., Costa, T. G., Szpoganicz, B., & Fávere, V. T. (2010). Adsorption and desorption of Cu(II), Cd(II) and Pb(II) ions using chitosan crosslinked with epichlorohydrin-triphosphate as the adsorbent. *Journal of Hazardous Materials*, *183*, 233–241.
- Li, X. G., Ma, X. L., Sun, J., & Huang, M. R. (2009). Powerful reactive sorption of silver(I) and mercury(II) onto poly(o-phenylenediamine) microparticles. *Langmuir*, *25*, 1675–1684.
- Liu, C., Bai, R., & Hong, L. (2006). Diethylenetriamine-grafted poly(glycidylmethacrylate) adsorbent for effective copper ion adsorption. *Journal of Colloids Interface Science*, *303*, 99–108.
- Liu, W., Zhang, J., Zhang, C., Wang, Y., & Li, Y. (2010). Adsorptive removal of Cr (VI) by Fe-modified activated carbon prepared from *Trapa natans* husk. *Chemical Engineering Journal*, *162*, 677–684.

- Lu, Q. F., Huang, M. R., & Li, X. G. (2007). Synthesis and heavy-metal-ion sorption of pure sulfophenylenediamine copolymer nanoparticles with intrinsic conductivity and stability. *Chemistry-A European Journal*, *13*, 6009–6018.
- Mansri, A., Benabadji, K. I., Desbrières, J., & François, J. (2009). Chromium removal using modified poly(4-vinylpyridinium) bentonite salts. *Desalination*, *245*, 95–107.
- Moussavi, G., & Barikbin, B. (2010). Biosorption of chromium (VI) from industrial wastewater onto pistachio hull waste biomass. *Chemical Engineering Journal*, *162*, 893–900.
- Mustafa, S., Ahmad, T., Naeem, A., Shah, K. H., & Waseem, M. (2010). Kinetics of chromium ion removal from tannery wastes using amberlite IRA-400 Cl⁻ and its hybrids. *Water, Air, and Soil Pollution*, *210*, 43–50.
- Namasivayam, C., & Kavita, D. (2002). Removal of congo red from water by adsorption on to activated carbon prepared from coir pith, an agricultural solid waste. *Dyes and Pigments*, *54*, 47–58.
- Nastasovic, A., Sandic, Z., Surucic, L., Maksin, D., Jakovljevic, D., & Onjia, A. (2009). Kinetics of hexavalent chromium sorption on amino-functionalized macroporous glycidyl methacrylate copolymer. *Journal of Hazardous Materials*, *171*, 153–159.
- Osman, B., Kara, A., & Beşirli, N. (2011). Immobilization of glucoamylase onto Lewis metal ion chelated magnetic affinity sorbent: kinetic, isotherm and thermodynamic studies. *Journal of Macromolecular Science Pure & Applied Chemistry*, *A48*, 387–399.
- Owlad, M., Aroua, M. K., Ashri, W., Daud, W., & Baroutian, S. (2009). Removal of hexavalent chromium-contaminated water and wastewater: a review. *Water, Air, and Soil Pollution*, *200*, 59–77.
- Özcan, A., Özcan, A. S., Tunali, S., Akar, T., & Kiran, I. (2005). Determination of the equilibrium, kinetic and thermodynamic parameters of adsorption of copper(II) ions onto seeds of *Capsicum annuum*. *Journal of Hazardous Materials*, *124*, 200–208.
- Pişkin, E., Kesenci, K., Şatiroğlu, N., & Genç, Ö. (1996). Dithiocarbamate-incorporated monodisperse polystyrene microspheres as specific sorbents: adsorption of cadmium ions. *Journal of Applied Polymer Science*, *59*, 109–117.
- Plazinski, W., Rudzinski, W., & Plazinska, A. (2009). Theoretical models of sorption kinetics including a surface reaction mechanism: a review. *Advances in Colloid and Interface Science*, *152*, 2–13.
- Rao, R. A. K., & Rehman, F. (2010). Adsorption studies on fruits of Gular (*Ficus glomerata*): removal of Cr(VI) from synthetic wastewater. *Journal of Hazardous Materials*, *181*, 405–412.
- Restani, R. B., Correia, V. G., Bonifácio, V. D. B., & Ricardo, A. A. (2010). Development of functional mesoporous microparticles for controlled drug delivery. *Journal of Supercritical Fluids*, *55*, 333–339.
- Ritchie, A. G. (1977). Alternative to elovich equation for kinetics of adsorption of gases on solids. *Journal of the Chemical Society, Faraday Transactions*, *73*, 1650–1653.
- Rivas, B. L., Seguel, G. V., & Ancatripai, C. (2000). Polymer-metal complexes: synthesis, characterization, and properties of poly(maleic acid) metal complexes with Cu(II), Co (II), Ni(II), and Zn(II). *Polymer Bulletin*, *44*, 445–452.
- Safarik, I., & Safarikova, M. (2009). Magnetic nano- and micro-particles in biotechnology. *Chemical Papers*, *63*, 497–505.
- Safarik, I., & Safarikova, M. (2010). Magnetic affinity separation of recombinant fusion proteins. *Hacettepe Journal of Biology and Chemistry*, *38*, 1–7.
- Sağ, Y., & Kutsal, T. (2000). Determination of the biosorption activation energies of heavy metal ions on *Zoogloea ramigera* and *Rhizopus arrhizus*. *Process Biochemistry*, *35*, 801–807.
- Salih, B., Denizli, A., Kavaklı, C., Say, R., & Pişkin, E. (1998). Adsorption of heavy metal ions onto dithizone-anchored poly(EGDMA-HEMA) microbeads. *Talanta*, *46*, 1205–1213.
- Say, R., Garipcan, B., Emir, S., Patır, S., & Denizli, A. (2002). Preparation and characterization of the newly synthesized metal-complexing-ligand *N*-methacryloylhistidine having HEMA beads for heavy metal removal from aqueous solutions. *Macromolecular Materials and Engineering*, *287*, 539–545.
- Say, R., Tuncel, A., & Denizli, A. (2002). Adsorption of Ni²⁺ from aqueous solutions by novel polyethyleneimine-attached poly(p-chloromethylstyrene) beads. *Journal of Applied Polymer Science*, *83*, 2467–2473.
- Say, R., Birlık, E., Denizli, A., & Ersöz, A. (2006). Removal of heavy metal ions by dithiocarbamate-anchored polymer/organosmectite composites. *Applied Clay Science*, *31*, 298–305.
- Schulte, D. M., & Rode, T. S. (2006). Thermosensitive magnetic polymer particles as contactless controllable drug carriers. *Journal of Magnetism and Magnetic Materials*, *302*, 267–271.
- Şenel, S., Uzun, L., Kara, A., & Denizli, A. (2008). Heavy metal removal from synthetic solutions with magnetic beads under magnetic field. *Journal of Macromolecular Science Pure & Applied Chemistry*, *A45*, 635–642.
- Sharma, Y. C., Srivastava, V., Weng, C. H., & Upadhyay, S. N. (2009). Removal of Cr(VI) from wastewater by adsorption on iron nanoparticles. *Canadian Journal of Chemical Engineering*, *87*, 921–929.
- Szablewska, E. M., Safarikova, M., & Safarik, I. (2010). Magnetic studies of ferrofluid-modified microbial cells. *Journal of Nanoscience and Nanotechnology*, *10*, 2531–2536.
- Tassist, A., Lounici, H., Abdi, N., & Mameri, N. (2010). Equilibrium, kinetic and thermodynamic studies on aluminum biosorption by a mycelial biomass (*Streptomyces rimosus*). *Journal of Hazardous Materials*, *183*, 35–43.
- Tekin, N., Kadıncı, E., Demirbaş, Ö., Alkan, M., & Kara, A. (2006). Adsorption of polyvinylimidazole onto kaolinite. *Journal of Colloid and Interface Science*, *296*, 472–479.
- Tripathy, S. S., & Raichur, A. M. (2008). Abatement of fluoride from water using manganese dioxide-coated activated alumina. *Journal of Hazardous Materials*, *153*, 1043–1051.
- Üçer, A., Uyanık, A., & Aygün, Ş. F. (2006). Adsorption of Cu (II), Cd(II), Zn(II), Mn(II) and Fe(III) ions by tannic acid immobilised activated carbon. *Separation and Purification Technology*, *47*, 113–118.
- Uğuzdoğan, E., Denkbaş, E. B., Öztürk, E., Tuncel, S. A., & Kabasakal, O. S. (2009). Preparation and characterization of polyethyleneglycolmethacrylate (PEGMA)-co-vinylimidazole (VI) microspheres to use in heavy metal removal. *Journal of Hazardous Materials*, *162*, 1073–1080.

- Ünlü, N., & Ersoz, M. (2006). Adsorption characteristics of heavy metal ions onto a low cost biopolymer sorbent from aqueous solutions. *Journal of Hazardous Materials*, *B136*, 272–280.
- Unnithan, M. R., Vinod, V. P., & Anirudhan, T. S. (2004). Synthesis, characterization, and application as a chromium(vi) adsorbent of amine-modified polyacrylamide-grafted coconut coir pith. *Industrial and Engineering Chemistry Research*, *43*, 2247–2255.
- Uzdoğan, E., Denkbaş, E. B., & Kabasakal, O. S. (2010). The use of polyethylene glycolmethacrylate-co-vinylimidazole (PEGMA-co-VI) microspheres for the removal of nickel(II) and chromium(VI) ions. *Journal of Hazardous Materials*, *177*, 119–125.
- Wang, X. S., Tang, Y. J., Chen, L. F., Li, F. Y., Wan, W. Y., & Tan, Y. B. (2010). Removal of Cr(VI) by zero-valent, iron-encapsulated alginate beads. *Clean–Soil, Air, Water*, *38*, 263–267.
- Wu, F.-C., Tseng, R.-L., & Juang, R.-S. (2001). Kinetic modeling of liquid-phase adsorption of reactive dyes and metal ions on chitosan. *Water Research Volume*, *35*, 613–618.
- Yavuz, H., Denizli, A., Gungunes, H., Safarikova, M., & Safarik, I. (2006). Biosorption of mercury on magnetically modified yeast cells. *Separation and Purification Technology*, *52*, 253–260.
- Zhao, Y.-G., Shen, H.-Y., Pan, S.-D., & Hu, M.-Q. (2010). Synthesis, characterization and properties of ethylenediamine-functionalized Fe₃O₄ magnetic polymers for removal of Cr(VI) in wastewater. *Journal of Hazardous Materials*, *182*, 295–302.
- Zolgharnein, J., & Shahmoradi, A. (2010). Characterization of sorption isotherms, kinetic models, and multivariate approach for optimization of Hg(II) adsorption onto fraxinus tree leaves. *Journal of Chemical Engineering Data*, *55*, 5040–5049.